



Predicting cloud ice nucleation caused by atmospheric mineral dust

Slobodan Nickovic¹, Bojan Cvetkovic¹, Fabio Madonna², Goran Pejanovic¹, Slavko Petkovic¹ and Jugoslav Nikolic¹

5 ¹Republic Hydrometeorological Service of Serbia, 11000 Beograd, Serbia

²Consiglio Nazionale delle Ricerche, Istituto di Metodologie per l'Analisi Ambientale, 85050, Tito Scalo, Potenza, Italy

Correspondence to:

Dr. Slobodan Nickovic

10 Republic Hydrometeorological Service of Serbia,

11000 Beograd, Serbia

Phone +381-65-654-8154

E-mail: nickovic@gmail.com

15 **Keywords**

ice nucleation, model parameterization, dust aerosol

Abstract

Dust aerosols are very efficient ice nuclei important for heterogeneous cloud glaciation even in regions distant from
20 desert sources. A new generation of ice nucleation parameterizations, including dust as ice nucleation agent, opens the way
towards a more accurate treatment of cold cloud formation in atmospheric models. Using such parameterizations, we have
developed a regional dust-atmospheric modelling system capable to predict in real-time conditions dust-induced ice
nucleation. We executed the model with added ice nucleation component over the Mediterranean region, exposed to
moderate Saharan dust transport over two periods lasting 15 and 9 days, respectively. Model results are validated against
25 satellite and ground-based cloud-ice-related measurements, provided by SEVIRI (Spinning Enhanced Visible and InfraRed
Imager) and by the CNR-IMAA Atmospheric Observatory CIAO in Potenza, South Italy. Predicted ice nuclei concentration
shows reasonable level of agreement when compared against observed spatial and temporal patterns of cloud ice water. The
developed methodology permits to use ice nuclei as input into cloud microphysics schemes of atmospheric models,
expecting that this approach could improve predictions of cloud formation and associated precipitation.

30

1 Introduction

Aerosol acting as ice nucleating particles (n_{IN}) enhances the heterogeneous glaciation of cloud water making it to
freeze earlier and at higher temperatures than otherwise. Insoluble particles such as dust and biological particles are known



as the best ice nuclei. Cziczo et al (2013), hereinafter named CZ13, show that mineral dust and metallic oxide particles, found as residues in ice crystals of aircraft measurements over North and Central America, are prevailing (61%). Concerning the other aerosol types, CZ13 show that in such regions distant from dust sources, sea salt is represented only with 3% in regions out of the open ocean, whereas elemental carbon and biological particles appear with less than 1%. Furthermore, CZ13 demonstrate that the dominant ice nucleation (IN) is the heterogeneous immersion process in 94% of the collected samples. During IN, only a small number of dust particles, a few in a standard liter, is sufficient to trigger the cloud glaciation process at temperatures lower than -20°C (DeMott et al, 2010). Since dust with small concentrations is easily lifted to the mid and upper troposphere, cold clouds formed due to dust can be found at locations distant from dust deserts (Creamean et al 2013; CZ13).

Mineral dust particles can have a significant impact on IN and on associated cloud formation and precipitation (Sassen, 2005; DeMott et al., 2003; Yakobi-Hancock et al 2013). For example, measurement of ice residues from in-situ cold cloud samples and from precipitation measurements collected in California strongly suggest that non-soluble aerosol originated from Asia and Sahara dust sources (dust and biological aerosol) enhances ice formation in mid-level clouds and precipitation (Ault et al, 2011; Creamean et al 2013). Recent modelling experiments confirm that in the pristine environment dust and biological aerosol could increase the precipitation as well (Fan et al, 2014). In this process, there is little influence of dust chemical aging (DeMott et al., 2015).

Large interest on ice nucleation research, illustrated by the exponential growth of published articles in this field (DeMott et al, 2011) is motivated, inter alia, by needs of the community to improve unsatisfactory representation of cloud formation in atmospheric models, and therefore to increase the accuracy of weather and climate predictions. Older parameterizations (Fletcher, 1962; Meyers et al, 1992) considered n_{IN} as a function of temperature and ice saturation ratio only.

More recent observations however show that at a given temperature and moisture, n_{IN} depends on aerosol concentration as well. Based on this evidence, a new generation of n_{IN} parameterizations has been developed (DeMott et al, 2010; Niemand et al, 2012; Tobo et al., 2013; Phillips et al., 2013; Atkinson et al., 2013; DeMott et al, 2015), where dust is recognized as one of the major n_{IN} parameter.

Exploiting these findings, we have developed a coupled regional real-time forecasting atmosphere-dust forecasting system, which predicts n_{IN} affected by dust as an online model variable. Such new component represents a step towards operational cold clouds prediction and associated precipitation. To our knowledge, this is the first time that all ingredients needed for cold cloud formation by dust are predicted in operational forecasting mode within one modeling system. For this study, immersion and deposition modes of freezing are assumed to be dominant for ice formation process.

The model description and the implemented n_{IN} parameterizations are presented in Section 2. Observations used for the model evaluation and the model performance are presented in Sections 3. Comparisons of model simulations against observations are described in Section 4. Conclusions are given in Section 5.



2 Modelling

The evidence on dominant role of dust in cold cloud formation has motivated a number of research groups to link cloud microphysics schemes with parameterizations of dust-affected n_{IN} in atmospheric models. Atmospheric models which drive ice nucleation parameterizations are ranging from simplified 1-D and 1.5-D kinematic or trajectory models (Field et al. (2012; Eidhammer et al. 2010; Dearden et al. 2012; Simmel et al. 2015), to complex full atmospheric models (e.g. Niemand et al., 2012; Thompson and Eidhammer, 2014). However, only a few such models (used in weather and/or climate applications) have dust concentration as a forecasting parameter available for online n_{IN} calculation. For example, Niemand et al., (2012) studying a dust event, used temperature and dust particle surface area predicted by the regional-scale online coupled model COSMOART (Consortium for Small-Scale Modelling–Aerosols and Reactive Trace Gases) to calculate immersion freezing n_{IN} . The model has been validated only for a dust case episode using chamber-processed n_{IN} calculated from ground-based aerosol concentration measurements. Furthermore, Hande et al. (2015) have implemented the COSMO model coupled to MUlti-Scale Chemistry Aerosol Transport (MUSCAT) model to compute a seasonal variability of n_{IN} . This model has been validated against limited observation datasets (covering only a few weeks). A model which gets close to real-time forecasting of glaciated clouds is a ‘dust friendly’ version of the bulk microphysics scheme (Thompson and Eidhammer, 2014) with explicitly incorporates dust aerosol. However, this model currently uses a climatological rather than predicted dust concentration for n_{IN} calculations.

Following the objective of this study to develop a method for real-time n_{IN} prediction, we have used the Dust Regional Atmospheric Model (DREAM) driven by the National Centers for Environmental Predictions (NCEP) Nonhydrostatic Multiscale atmospheric Model on the E grid (NMME). Here, we have incorporated a parameterization of the ice nuclei concentration calculated at every model time step as a function of dust concentration and atmospheric variables. The predicted spatial and temporal distribution of n_{IN} represents the fraction of dust aerosol capable to produce mass of cloud water ice due to dust.

2.1 NMME model

NMME (Janjic et al., 2001, 2010; Janjic, 2003) has been used for various applications at NCEP and elsewhere since the early 2000s. From 2006 it has been the main operational short-range weather forecasting North American Model (NAM). It is also used for operational regional forecasts in the Republic Hydrometeorological Service of Serbia. The NMME dynamics core includes: energy/enstrophy horizontal advection; vertical advection; a nonhydrostatic add-on module; lateral diffusion; horizontal divergence damping; sub-grid gravity waves; transport of moisture and different passive tracers. Concerning the model physics there are various optional modules: cloud microphysical schemes ranging from simplified ones suitable for mesoscale modeling to sophisticated mixed-phase physics for cloud resolving models; cumulus parameterizations; surface physics; planetary boundary layer and free atmosphere turbulence; and the atmospheric longwave



and shortwave radiation schemes. NMME uses a hybrid vertical coordinate with a terrain-following sigma in the lower atmosphere, and a pressure coordinate in the upper atmosphere.

2.2 DREAM model

DREAM (Nickovic et al, 2001; Nickovic 2004; Pejanovic et al, 2011) has been developed to predict the atmospheric dust process, including the dust emission, dust horizontal and vertical turbulent mixing, long-range transport and dust deposition. Eight radii bins in the model range from 0.15 μm to 7.1 μm . Dust emission parameterization includes a viscous sub-layer between the surface and the lowest model layer (Janjic, 1994) in order to parameterize the turbulent vertical transfer of dust into the lowest model layer following different turbulent regimes (laminar, transient and turbulent mixing). The wet dust removal is proportional to rainfall rate. Specification of dust sources is based on mapping of the areas that are dust productive under favourable weather conditions. The USGS land cover data combined with preferential dust sources of dust originating from sediments in paleo-lake and riverine beds (Ginoux et al., 2001) have been used to define barren and arid soils as dust-productive areas

2.3 Ice nucleation parameterization

In this study, dust concentration, atmospheric temperature and moisture as predicted by the atmospheric component of the coupled model are used to calculate. The n_{IN} parameterization consists of two parts applied to warmer and colder glaciated clouds.

For temperatures ranging in the interval (-36°C; -10°C), we have implemented the immersion ice nucleation parameterization developed by DeMott et al. (2015):

$$n_{IN} = C(n_{dust})^{(\alpha(273.16-T)+\beta)} \exp(\gamma(273.16-T)+\delta) \quad (1)$$

where n_{IN} is the number concentration of ice nuclei [l^{-1}]; n_{dust} is the number concentration of dust particles with diameter larger than 0.5 μm [cm^{-3}]; T is the temperature in Celsius degrees; $\alpha=0$; $\beta=1.25$; $\gamma = 0.46$; and $d = -11.6$. Equation (1) is applied when relative humidity with respect to ice is exceeding 100%. This parameterization scheme has been developed as an extension of DeMott et al. (2010) and Tobo et al. (2013), but applied exclusively to mineral dust n_{IN} collected in laboratory and field measurements. With the DeMott et al (2015) approach, the spread of errors in predicting IN concentrations at a given temperature has been reduced from a factor of ~ 1000 to ~ 10 . Their parameterization is based on use of observations from a number of field experiments at a variety of geographic locations over a period longer than a decade, demonstrating that there is a correlation between the observed n_{IN} and the dust number concentrations of particles larger than 0.25 μm radius. In DeMott et al. (2015), $C=3$ is chosen as a calibration factor to adjust the scheme to dust measurements. The parameterization is extrapolated down to -5°C despite the fact that the underlying measurements were only taken at temperatures lower than -9°C.



For temperatures ranging in the interval (-55°C; -36°C), we have implemented the Steinke et al. (2015) parameterization for the deposition ice nucleation based on the ice nucleation active surface site approach in which n_{IN} is a function of temperature, humidity and the aerosol surface area concentration. In the deposition nucleation, water vapor is directly transformed into ice at the particle's surface, occurring at the time of or shortly after the water condensation on the particle, which acts at the same time as condensation and freezing nuclei. For deposition nucleation, water vapor is directly transformed into ice at the particle's surface. Steinke et al. (2015) calculate the number concentration of ice nuclei due to deposition freezing as:

$$n_{IN} = pS_{dust} \exp[-q(T - 273.16) + (rRH_{ice} - 100)] \quad (2)$$

here n_{IN} is the number concentration of ice nuclei [cm^{-3}]; S_{dust} is ice nucleation active surface [m^{-2}] linked to dust concentration (Niemand et al. 2012); $p = 188 \times 10^5$; $q = -1.0815$; $r = -0.815$; T is temperature in degrees Celsius; RH_{ice} is relative humidity with respect to ice. In our experiments, RH_{ice} is pre-specified to the value of 110%.

Although based on two different parameterizations, the resulting n_{IN} has a smooth transition across the temperature boundary of -36°C between the DeMott et al. (2015) and Steinke et al. (2015) scheme, as our model results shown later demonstrate. Therefore, there was no need to numerically smooth n_{IN} of the two schemes to secure appropriate matching.

15 3 Observations

The model capabilities to predict vertical features of dust and cold clouds have been evaluated using vertical profiles of the aerosol and cloud properties routinely measured at the CNR-IMAA Atmospheric Observatory (CIAO) at Tito Scalo (Potenza), Italy, using several ground-based remote sensing techniques, like lidar, radar and passive techniques. Multi-wavelength Raman lidar measurements allow to monitor the dynamical evolution in troposphere of the aerosol particles, but also to identify the different aerosol types (Papagiannopoulos et al., 2015) taking advantage of the large number optical properties they are able to provide, i.e. lidar ratio at two wavelengths, the Angstrom exponent, the backscatter-related Angstrom exponent, and linear particle depolarization ratio. This aerosol typing capability allows to classify the aerosol type acting n_{IN} , and especially to separate mineral dust from other types of aerosol.

CIAO, as one of the Cloudnet stations (www.cloud-net.org), applies the Cloudnet retrieval scheme to provide vertical profiles of cloud types. Cloudnet processing is based on the use of ceilometer, microwave radiometer and cloud radar observations. For the CIAO station (Madonna et al., 2010; Madonna et al., 2011), the Cloudnet processing involves observations provided by the VAISALA CT25k ceilometer, the Radiometrics MP3014 microwave profiler, and the METEK millimeter-wavelength Doppler and polarimetric cloud radar MIRA36. MIRA36 is a 3D scanning system, but for Cloudnet processing makes use of zenith pointing observations only.

Cloudnet processing provides a categorization of the observed vertical profiles of cloud water categories, such as liquid droplets, ice particles, aerosols and insects. This categorization is essentially based on different sensitivities of lidar and radar to different particle size ranges. For layers identified as ice clouds, the ice water content (with the related uncertainty) is derived from radar reflectivity factor and air temperature using an empirical formula based on dedicated



aircraft measurements (Hogan et al., 2005). Consistency between Cloudnet products and Raman lidar observations performed at CIAO of clouds has been also checked (Rosoldi et al., 2016).

To complement the Potenza in-situ profiling observations and to examine how the model predicts horizontal distribution of cold clouds, the MSG/SEVIRI ice water path satellite observations are used. SEVIRI (the Spinning Enhanced Visible and InfraRed Imager), as a geostationary passive imager, is on board of the Meteosat Second Generation (MSG) systems. High SEVIRI spatial and temporal resolution (~4km and 15min, respectively) provides, among other, high-quality products. Input to the retrieval schemes were inter-calibrated effective radiances of Meteosat-8 and 9. In our study, daily averages of the retrieved ice water path of the SEVIRI cloud property dataset (CLAAS) are used (Stengel et al., 2013a; Stengel et al., 2013b) to validate the model on the regional scale:

$$IWP = \frac{2}{3} r_i r_{eff} \tau$$

Here, IWP [gm^{-2}] is the ice water path, τ is the vertically integrated cloud optical thickness at $0.6\mu m$ derived in satellite pixels assigned to be cloud filled; r_{eff} is the surface-area-weighted radius of cloud particles [μm]; $r_i = 0.93gcm^{-3}$ is the ice water density.

4 Model experiments and validation

The model domain covers Northern Africa, Southern Europe and the Mediterranean. The model resolution has been set to 25km in the horizontal, and to 28 layers in the vertical ranging from the surface to 100hPa. The initial and boundary atmospheric conditions for the NMME model have been updated every 24 hours using the ECMWF 0.5deg analysis data. The concentration is set to zero at the 'cold start' of DREAM launched 4 days before the period to be studied, permitting so the model to be 'warmed-up', i.e. to develop meaningful concentration field at a date considered as an effective model start. After that time point, 24-hour dust concentration forecasts from the previous-day runs have been declared as initial states for the next-day run of DREAM.

The coupled NMME-DREAM model has been run and validated against ground-based and satellite observations for two periods (1-15 May 2010, and 20-29 September 2012) during which the CIAO Potenza instruments have observed occasional occurrence of Saharan dust accompanied with sporadic formation of mixed-phase and/or cold clouds. These periods characterized by modest rather than major dust transport into the Mediterranean have been intentionally chosen to learn if non-intensive dust conditions still can form cold clouds.

For the May 2010 period, a detailed day-by-day comparison of the model against SEVIRI data is shown in Figure 1. It is important to mention that during the periods 8–9 May and 13–14 May, the Eyjafjallajökull volcanic cloud has been also observed in Potenza (Mona et al, 2012; Pappalardo et al, 2013), thus potentially interfering with dust. Eventual influences of the existing volcanic ash on our results are commented later.

Figure 1 shows mapped daily averages of the following variables: the model vertical dust load (DL), the model $NL = \log_{10} \int n_{IN} dz$, the MSG-SEVIRI IWPL= $\log_{10}(IWP)$, and the overlap of NL and IWPL; columns in the Figure



showing these variables are marked by A, B C and D, respectively. From columns (A) and (B) in the Figure 1 one can observe general lack of coincidence between DL and NL. This difference is expected, since the cold cloud formation is dependent not only on dust but also on its complex interaction with the atmospheric thermodynamical conditions. On the other hand, a visual inspection shows considerable similarity between NL and the IWPL patterns (columns (B) and (C)) with respect to their shapes and locations.

Maps in column (D) show how much the normalized NL and IWPL daily averages are overlapped. Hits, misses and false alarms are represented by areas shaded in blue, green and brown color, respectively. One can notice that the overlapping (hits) always represents the largest parts of the shown daily maps. Although not dominant, there are however certain regions of cold clouds either observed but not predicted (misses), or predicted but not observed (false alarms). The former case should not necessarily be erroneous because it might be addressed the processes not represented by our parameterization: to clouds generated by homogeneous glaciation or to clouds made by heterogeneous freezing with aerosols other than dust.

To gain additional evidence on matching between NL and IWPL, we used their normalized daily averages to calculate the following statistical dichotomous (yes/no) scores based on hits, misses and correct negatives (not predicted, not observed) (WMO, 2009):

- accuracy - showing what fraction of the forecasts were correct;
- probability of detection (hit rate) - showing what fraction of the observed "yes" events were correctly forecasted;
- the false alarm ratio - showing what fraction of the predicted "yes" events actually did not occur.

Scores are calculated using values for all model/observation grid points and for all days of the considered period. Figure 2 shows the time evolution of the scores (which by definition range between 0 and 1). In average for the whole period, 63.4% of all NL were correct with respect to IWPL, 73.9% of the observed IWPL were predicted, and for 30.4% of the forecast NL, IWPL was not observed. Such result confirms high matching level between two fields shown in Figure 1.

In order to additionally illustrate the level of matching between NL and IWPL, we have further selected one day of the considered May 2010 period to which we have applied the contiguous rain area (CRA) technique (Ebert and McBride, 2000; Ebert and Gallus, 2009) introduced in numerical weather prediction for verifying the accuracy of precipitation forecasts; the method is sufficiently general so that could be applied to other geophysical fields as well. To make CRA applicable for our analysis where there are two different physical variables, we use the normalized NL and IWPL whose patterns are compared. To match the forecast and observed entities within a CRA, the forecasts are translated horizontally over the observations until the minimum squared error (MSE) is achieved. The translation vector calculated by CRA represents the location error of the forecast. Finally, with user predefined thresholds of two compared entities, CRA decomposes MSE into three components: the displacement error, the volume error, and the pattern error. As an example of the CRA pattern matching, we show results of the technique applied to 11 May 2010 normalized daily-averaged IWPL and



NL fields (Figure 3). CRA recognizes two best matching pairs of entities (shaded in red and green colours), dominating over other are smaller-scale patterns.

To evaluate the model performance in representing the vertical structure of the ice water clouds, n_{IN} have been compared with observed IWC obtained using the Cloudnet retrieval scheme over Potenza. Figure 4 shows time evaluation
5 $\log_{10}(n_{IN})$ (coloured shaded) and $\log_{10}(\text{IWC} \times 10^{-6} \frac{\text{kg}}{\text{m}^3})$, (contour plotted) over periods 1-15 May 2010 and 22-30 September 2012. In addition, red contours show the temperature field as provided by the NMME model. The different quantities provided by DREAM and Cloudnet to characterize the cloud ice content makes the comparison less punctual on a quantitative basis. Anyhow, in order to predict IWC we need to incorporate predicted n_{IN} into a cloud microphysics scheme, which is a future task of our project. Therefore, the comparison using a semi-quantitative approach is the only available at
10 the current stage of the analysis.

The comparisons reveal good performances of DREAM in predicting the vertical structure of the observed ice clouds. On 1-15 May 2010, a remarkable agreement between the ice vertical layer retrieved using the cloud radar observation and those predicted by the model is noted, though the model underpredicts the vertical extent of the ice layer over most of the time series. Most of the ice, observed by the cloud radar below 4.0-4.5 km above ground level (AGL), is not
15 predicted by the model. This is particularly evident on 6 May when only ice cloud layer below 3 km AGL is observed by the radar, but completely missed by the model.

On 22-30 September 2012 the model is able to catch the deep ice layers observed on 25-27 September 2012 between about 5 and 12 km AGL (-10°C and -60°C) and it is able to partially predict a part of the thinner layers observed after 27 September above 7 km AGL ($<-25^{\circ}\text{C}$). The model is also able to well predict the cirrus clouds observed by the cloud
20 radar on 29 September in the range between 6 and 12 km. It is also worth to mention that co-located and simultaneous Raman lidar measurements (not reported) show some high optically thin cloudiness not detected by the radar because of its limited sensitivity to thin clouds at that height levels (Borg et al., 2013). In particular, this is the case of the layers predicted by the model in the second half of 27 September and on 28 September in the range between 9 and 12 km. Moreover, like for the case of May 2010, the model tends to underpredict the lowest ice water layers observed with the radar below 4.5 km
25 AGL.

In Figure 5 we also report the comparison of IWPL and NL over Potenza calculated every three hours, in the period from 1 to 15 May 2010 (upper panel) and from 22 to 30 September 2012 (lower panel). The outcome of the comparison confirms the good performance of the model in the prediction of the ice clouds over the whole atmospheric column.

The correlation between the IWPL and NL retrieved using ground based measurements merging datasets from both
30 the selected cases studies of 1-15 May 2010 and 22-30 September 2012 is shown in Figure 6. Linear correlation made considering the daily averaged for both the quantities provides a regression coefficient of $R=0.83$. The scatter plot shows a large variability in the values corresponding to higher values of the IWP and to the higher values of IL. Therefore, for



optically thinner ice clouds, IL linearly increases with IWPL. For larger IWPL values, the two variables are less correlated and second or higher order polynomial fitting could compromise the linear relationship.

In the period between 13-15 May 2010, both DREAM and back trajectories analysis showed that, while the transport of volcanic aerosol from Iceland (due to the Eruption of volcano Eyjafjalla 2010) was still ongoing, dust contribution was not negligible (Mona et al., 2012). In this period, the volcanic aerosol was mainly transported across the Atlantic Ocean, passing over Ireland and west UK, and then transported to the west off the Iberian Peninsula before reaching the Mediterranean Basin and Southern Italy. Satellite images and ground-based measurements confirmed the presence of volcanic particles in the corresponding regions (not shown). The analysis of multi-wavelength Raman lidar measurements permitted a detailed aerosol typing at the different altitude levels over Europe. A detailed description of lidar measurements performed by EARLINET (European Aerosol Research Lidar NETWORK) over Europe during this period was reported in Pappalardo et al., (2014).

The Iberian Peninsula, France and South Italy were the regions more significantly affected by the presence of volcanic aerosol (sulphate and small ash) during the considered period. For the purpose of our modelling study this might induce an underestimation of the IN (since IN due to dust only is modelled) in the above mentioned regions and can be responsible of part of the discrepancies between modelled IN and IWP provided by SEVIRI. This is particularly true for Iberian Peninsula where volcanic aerosol concentrations were quite relevant. The comparison of model predicted IN and SEVIRI IWC on 13 May shows differences that might be correlated to a larger availability of IN of volcanic origin.

On the contrary, in South Italy, the volcanic layer, observed at Potenza up to an altitude of about 8 km above sea level, did not enhance the formation of cold clouds due to unfavourable dry conditions in the free troposphere; this is also confirmed by the Potenza cloud radar which did not observe clouds for the whole day (Figure 4). The absence of cold clouds over most of South Italy, including Potenza region, is also shown by the IWC reported for 13 May in Figure 1.

5 Conclusions

We have extended the regional DREAM-NMME modelling system with the on-line parameterization of heterogeneous ice nucleation caused by mineral dust aerosol. We employed recently developed empirical parameterizations for immersion and deposition ice nucleation that include dust concentration as a dependent variable for cloud glaciation process. In our approach, ice nucleation concentration is calculated as a prognostic parameter depending on dust and atmospheric thermodynamic conditions. The model was applied for the Mediterranean region and surroundings for two periods: 1-15 May 2010 and 22-30 September 2012 during which several dust transport events of moderate intensity occurred. The model has been validated against both ground-based and satellite observations for two periods with the aim to check the performance over both the horizontal and vertical cross-sections of the investigated atmosphere providing promising results. Somewhat lower performance of the model in representing ice layers at lower altitudes could be affected by capability of the parameterization scheme to predict mixed-phase clouds in the zone of warmer negative temperatures.



Our study aimed to develop a methodology which prepares a terrain for further improvement of predicting clouds and associated precipitation in current atmospheric models. Namely, operational numerical weather prediction systems today usually do not include aerosol effects in cloud formation or do it in a simplistic way. By integrating dust and atmospheric components into an unfired modelling system we achieved to have at every time step all necessary ingredients - atmospheric and aerosol parameters - to calculate ice nuclei concentration formed by dust, which will be used in our future development phase as input into a dust-friendly cloud microphysics to predict ice mixing ratio.

Acknowledgments

We acknowledge the EUMETSAT for use of its Satellite Application Facility on Climate Monitoring (CM SAF) data. The support for the modeling part of the study is provided by the Republic Hydrometeorological Service of Serbia; the support for the part of the study related to observation is provided by CNR-IMAA, EARLINET under EU grant RICA 025991 in the Sixth Framework Programme, and ACTRIS through EU Seventh Framework Programme (FP7/2007-2013) under grant 262254 (Including ACTRIS TNA).

References

- Allen, S. K., Boschung, J., Nauels, A., Xia, Y., Bex, V., and Midgley, P. M., Cambridge University Press, Cambridge, UK and New York, NY, USA, 2013.
- Atkinson, J. D., Murray, B. J., Woodhouse, M. T., Whale, T. F., Baustian, K. J., Carslaw, K. S., Dobbie, S., O'Sullivan, D., and Malkin, T. L.: The importance of feldspar for ice nucleation by mineral dust in mixed-phase clouds, *Nature*, 498, 355–358, 2013.
- Ault, A. P., Williams, C. R., White, A. B., Neiman, P. J., Creamean, J. M., Gaston, C. J., Ralph, F. M., and Prather, K. A.: Detection of Asian dust in California orographic precipitation, *J. Geophys. Res.-Atmos.*, 116, doi:10.1029/2010JD015351, 2011.
- Borg, L. A., R. E. Holz, and D. D. Turner (2011), Investigating cloud radar sensitivity to optically thin cirrus using collocated Raman lidar observations, *Geophys. Res. Lett.*, 38, L05807, doi:10.1029/2010GL046365.
- Creamean, J. M., Ault, A. P., White, A. B., Neiman, P. J., Ralph, F. M., Minnis, P., and Prather, K. A.: Impact of interannual variations in sources of insoluble aerosol species on orographic precipitation over California's central Sierra Nevada, *Atmos. Chem. Phys.*, 15, 6535-6548, doi:10.5194/acp-15-6535-2015, 2015.



- Dearden, C., Connolly, P. J., Choulaton, T., Field, P. R., and Heymsfield, A. J.: Factors influencing ice formation and growth in simulations of a mixed-phase wave cloud, *J. Adv. Model. Earth Syst.*, 4, M10001, doi:10.1029/2012MS000163, 2012.
- 5 DeMott, P. J., K. Sassen, M. R. Poellot, D. Baumgardner, D. C. Rogers, S. D. Brooks, A. J. Prenni, and S. M. Kreidenweis (2003), African dust aerosols as atmospheric ice nuclei, *Geophys. Res. Lett.*, 30(14), 1732, doi:10.1029/2003GL017410.
- DeMott, P.J., Prenni, A. J., Liu, X., Petters, M. D., Twohy, C. H., Richardson, M. S., Eidhammer, T., Kreidenweis, S. M., and Rogers, D. C.: Predicting global atmospheric ice nuclei distributions and their impacts on climate, *P. Natl. Acad. Sci. USA*, 107, 11217–11222, 2010.
- 10 DeMott, P. J., Möhler, O., Stetzer, O., Vali, G., Levin, Z., Petters, et al: Resurgence in ice nuclei measurement research, *B. Am. Meteorol. Soc.*, 92, 1623–1635, doi:10.1175/2011BAMS3119.1, 2011.
- 15 DeMott, P. J., Prenni, A. J., McMeeking, G. R., Sullivan, R. C., Petters, M. D., Tobo, Y., Niemand, M., Möhler, O., Snider, J. R., Wang, Z., and Kreidenweis, S. M.: Integrating laboratory and field data to quantify the immersion freezing ice nucleation activity of mineral dust particles, *Atmos. Chem. Phys.*, 15, 393-409, doi:10.5194/acp-15-393-2015, 2015.
- Ebert, E.E., McBride, J.L., 2000. Verification of precipitation in weather systems: Determination of systematic errors. *J. Hydrol.* 239,179–202.
- 20 Ebert, E.E., Gallus, W.A., 2009. Toward better understanding of the contiguous rain area (CRA) verification method for spatial verification. *Weather Forecast.* 24, 1401–1415.
- 25 Eidhammer, T., DeMott, P. J., Prenni, A. J., Petters, M. D., Twohy, C. H., Rogers, D. C., Stith, J., Heymsfield, A., Wang, Z., Pratt, K. A., Prather, K. A., Murphy, S. M., Seinfeld, J. H., Subramanian, R., and Kreidenweis, S. M.: Ice Initiation by Aerosol Particles: Measured and Predicted Ice Nuclei Concentrations versus Measured Ice Crystal Concentrations in an Orographic Wave Cloud, *J. Atmos. Sci.*, 67, 2417–2436, 2010.
- 30 Fan, J., Leung, L. R., DeMott, P. J., Comstock, J. M., Singh, B., Rosenfeld, D., Tomlinson, J. M., White, A., Prather, K. A., Minnis, P., Ayers, J. K., and Min, Q.: Aerosol impacts on California winter clouds and precipitation during CalWater 2011: local pollution versus long-range transported dust, *Atmos. Chem. Phys.*, 14, 81-101, doi:10.5194/acp-14-81-2014, 2014.



- Field, P. R., Heymsfield, A. J., Shipway, B. J., DeMott, P. J., Pratt, K. A., Rogers, D. C., Stith, J., and Prather, K. A.: Ice in Clouds Experiment-Layer Clouds, Part II: Testing Characteristics of Heterogeneous Ice Formation in Lee Wave Clouds, *J. Atmos. Sci.*, 69, 1066–1079, 2012.
- 5 Fletcher, N. H.: *The Physics of Rainclouds*, 390 pp., Cambridge Univ. Press, Cambridge, UK, 1962.
- Hogan, R. J., M. P. Mittermaier and A. J. Illingworth, 2005: The retrieval of ice water content from radar reflectivity factor and temperature and its use in the evaluation of a mesoscale model. *Q. J. R. Meteorol. Soc.*, in press.
- 10 IPCC, 2014: *Climate Change 2014: Synthesis Report. Contribution of Working Groups I, II and III to the Fifth Assessment Report of the Intergovernmental Panel on Climate Change* [Core Writing Team, R.K. Pachauri and L.A. Meyer (eds.)]. IPCC, Geneva, Switzerland, 151 pp.
- Kondo, Y., Liao, H., Lohmann, U., Rasch, P., Satheesh, S. K., Sherwood, S., Stevens, B., and Zhang, X. Y.: Clouds and aerosols, in: *Climate Change 2013: The Physical Science Basis. Contribution of Working Group I to the Fifth Assessment Report of the Intergovernmental Panel on Climate Change*, edited by: Stocker, T. F., Qin, D., Plattner, G.-K., Tignor, M.,
- 15 Madonna, F., A. Amodeo, G. D'Amico, L. Mona, and G. Pappalardo (2010), Observation of non-spherical ultragiant aerosol using a microwave radar, *Geophys. Res. Lett.*, 37, L21814, doi:10.1029/2010GL044999.
- 20 Madonna, F., Amodeo, A., Boselli, A., Cornacchia, C., Cuomo, V., D'Amico, G., Giunta, A., Mona, L., and Pappalardo, G.: CIAO: the CNR-IMAA advanced observatory for atmospheric research, *Atmos. Meas. Tech.*, 4, 1191-1208, doi:10.5194/amt-4-1191-2011, 2011.
- 25 Meyers, M. P., DeMott P. J., and Cotton, W. R.: New primary ice nucleation parameterizations in an explicit cloud model, *J. Appl. Meteor.*, 31, 708–721, 1992.
- Mona, L., Amodeo, A., D'Amico, G., Giunta, A., Madonna, F., and Pappalardo, G.: Multi-wavelength Raman lidar observations of the Eyjafjallajökull volcanic cloud over Potenza, southern Italy, *Atmos. Chem. Phys.*, 12, 2229-2244,
- 30 doi:10.5194/acp-12-2229-2012, 2012.
- Niemand, M., Moehler, O., Vogel, B., Vogel, H., Hoose, C., Connolly, P., Klein, H., Bingemer, H., DeMott, P., Skrotzki, J., and Leisner, T.: Parameterization of immersion freezing on mineral dust particles: An application in a regional scale model, *J. Atmos. Sci.*, 69, 3077–3092, 2012.



- Nickovic, S., (2005), Distribution of dust mass over particle sizes: impacts on atmospheric optics, Forth ADEC Workshop - Aeolian Dust Experiment on Climate Impact, 26-28 January, Nagasaki, Japan, 357-360.
- 5 O'Sullivan, D., Murray, B. J., Malkin, T. L., Whale, T. F., Umo, N. S., Atkinson, J. D., Price, H. C., Baustian, K. J., Browse, J., and Webb, M. E.: Ice nucleation by fertile soil dusts: relative importance of mineral and biogenic components, Atmos. Chem. Phys., 14, 1853-1867, doi:10.5194/acp-14-1853-2014, 2014
- Boucher, O., Randall, D., Artaxo, P., Bretherton, C., Feingold, G., Foster, P., Kerminen, V.-M.,
- 10 Pappalardo, G., et al.: Four-dimensional distribution of the 2010 Eyjafjallajökull volcanic cloud over Europe observed by EARLINET, Atmos. Chem. Phys., 13, 4429-4450, doi:10.5194/acp-13-4429-2013, 2013.
- Pejanovic, G., S. Nickovic, M. Vujadinovic, A. Vukovic, V. Djurdjevic, M. Dacic, Atmospheric deposition of minerals in dust over the open ocean and possible consequences on climate. WCRP OSC Climate Research in Service to Society, 24-28
- 15 October 2011, Denver, CO, USA
- Phillips, V. T. J., DeMott, P. J., Andronache, C., Pratt, K., Prather, K. A., Subramanian, R., and Twohy, C.: Improvements to an Empirical Parameterization of Heterogeneous Ice Nucleation and its Comparison with Observations, J. Atmos. Sci., 70, 378-409, 2013.
- 20 Sassen, K. (2005), Dusty ice clouds over Alaska, Nature, 434, 456.
- Simmel, M., Bühl, J., Ansmann, A., and Tegen, I.: Ice phase in altocumulus clouds over Leipzig: remote sensing observations and detailed modeling, Atmos. Chem. Phys., 15, 10453-10470, doi:10.5194/acp-15-10453-2015, 2015.
- 25 Steinke, I., Hoose, C., Möhler, O., Connolly, P., and Leisner, T.: A new temperature- and humidity-dependent surface site density approach for deposition ice nucleation, Atmos. Chem. Phys., 15, 3703-3717, doi:10.5194/acp-15-3703-2015, 2015.
- Stengel, M., Kniffka, A., Meirink, J. F., Lockhoff, M., Tan, J., and Hollmann, R.: CLAAS: the CM SAF cloud property data
- 30 set using SEVIRI, Atmos. Chem. Phys., 14, 4297-4311, doi:10.5194/acp-14-4297-2014, 2014.
- Stengel, Martin; Kniffka, Anke; Meirink, Jan Fokke; Riihelä, Aku; Trentmann, Jörg; Müller, Richard; Lockhoff, Maarit; Hollmann, Rainer: CLAAS: CM SAF CLOUD property dAtaset using SEVIRI - Edition 1 - Hourly / Daily Means, Pentad



Means, Monthly Means / Monthly Mean Diurnal Cycle / Monthly Histograms. Satellite Application Facility on Climate Monitoring, 2013b. DOI:10.5676/EUM_SAF_CM/CLAAS/V001. http://dx.doi.org/10.5676/EUM_SAF_CM/CLAAS/V001

Thompson, G., P. R. Field, R. M. Rasmussen, and W. D. Hall, 2008: Explicit forecasts of winter precipitation using an improved bulk microphysics scheme. Part II: Implementation of a new snow parameterization. *Mon. Wea. Rev.*, 136, 5095–5115, doi:10.1175/2008MWR2387.1

Thompson, G and T.Eidhammer, 2014: A Study of Aerosol Impacts on Clouds and Precipitation Development in a Large Winter Cyclone. *J. Atmos. Sci.*, 71, 3636–3658.

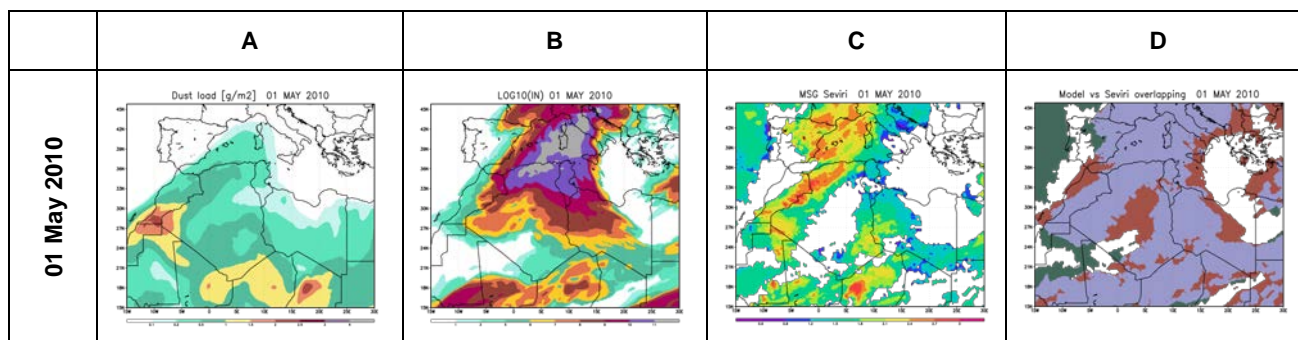
10

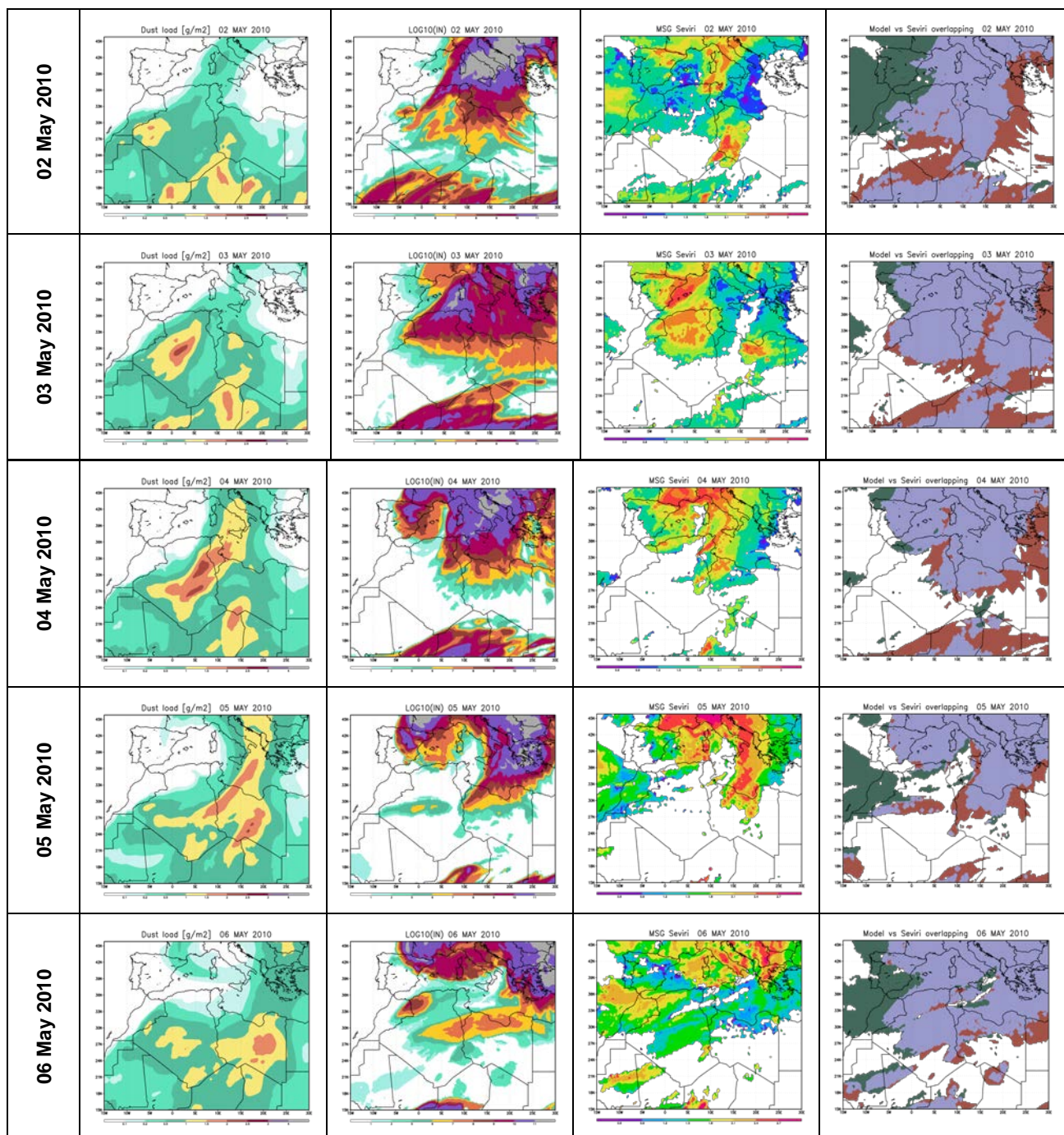
Tobo, Y., Prenni, A. J., DeMott, P. J., Huffman, J. A., McCluskey, C. S., Tian, G., Pöhlker, C., Pöschl, U., and Kreidenweis, S. M.: Biological aerosol particles as a key determinant of ice nuclei populations in a forest ecosystem, *J. Geophys. Res.-Atmos.*, 118, 10100–10110, doi:10.1002/jgrd.50801, 2013.

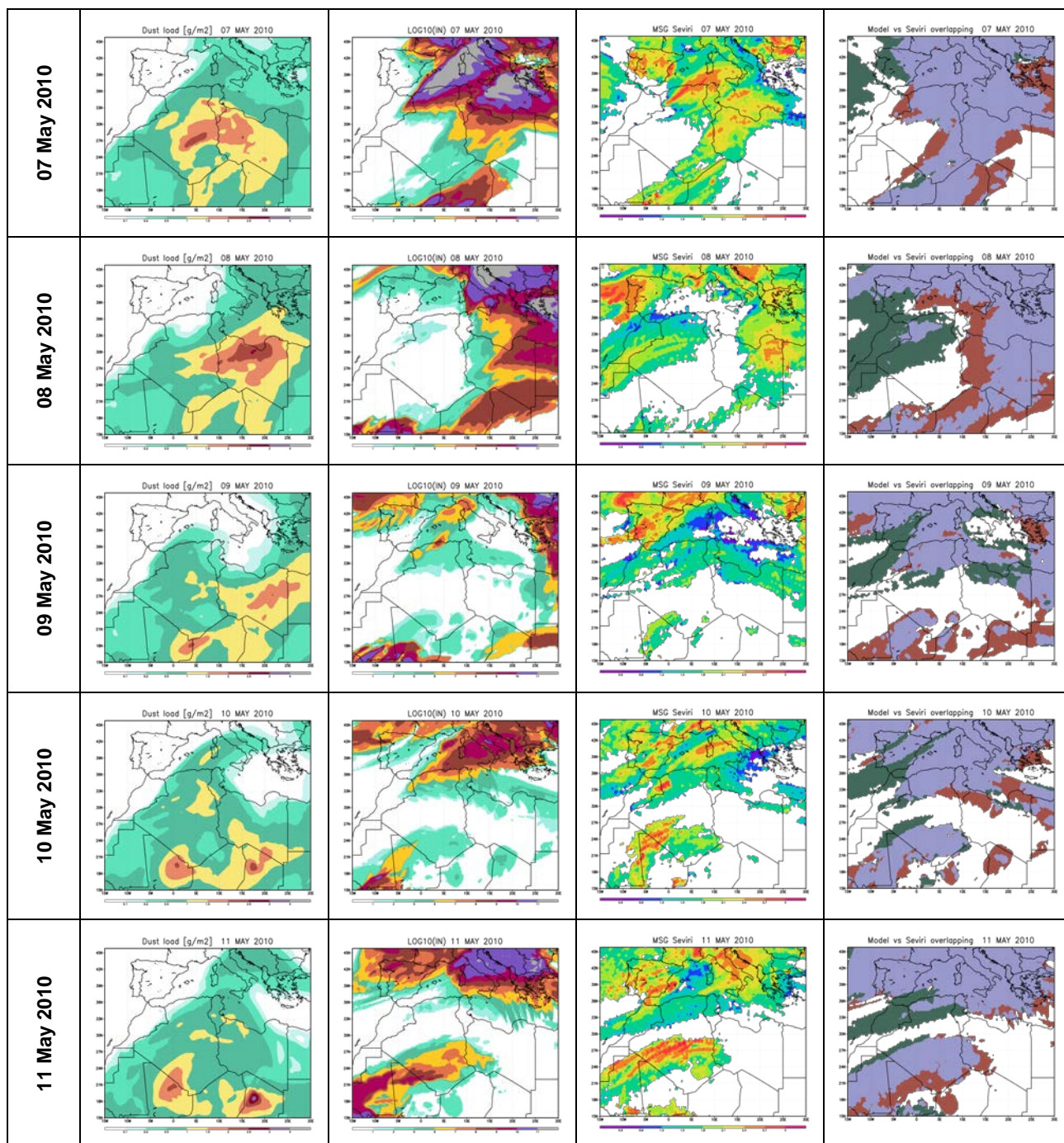
15 WMO, 2009: Recommendations for the Verification and Intercomparison of QPFs and PQPFs from Operational NWP Models (Revision 2, October 2008) (WMO TD No 1485) (WWRP 2009-1)

Figures

20







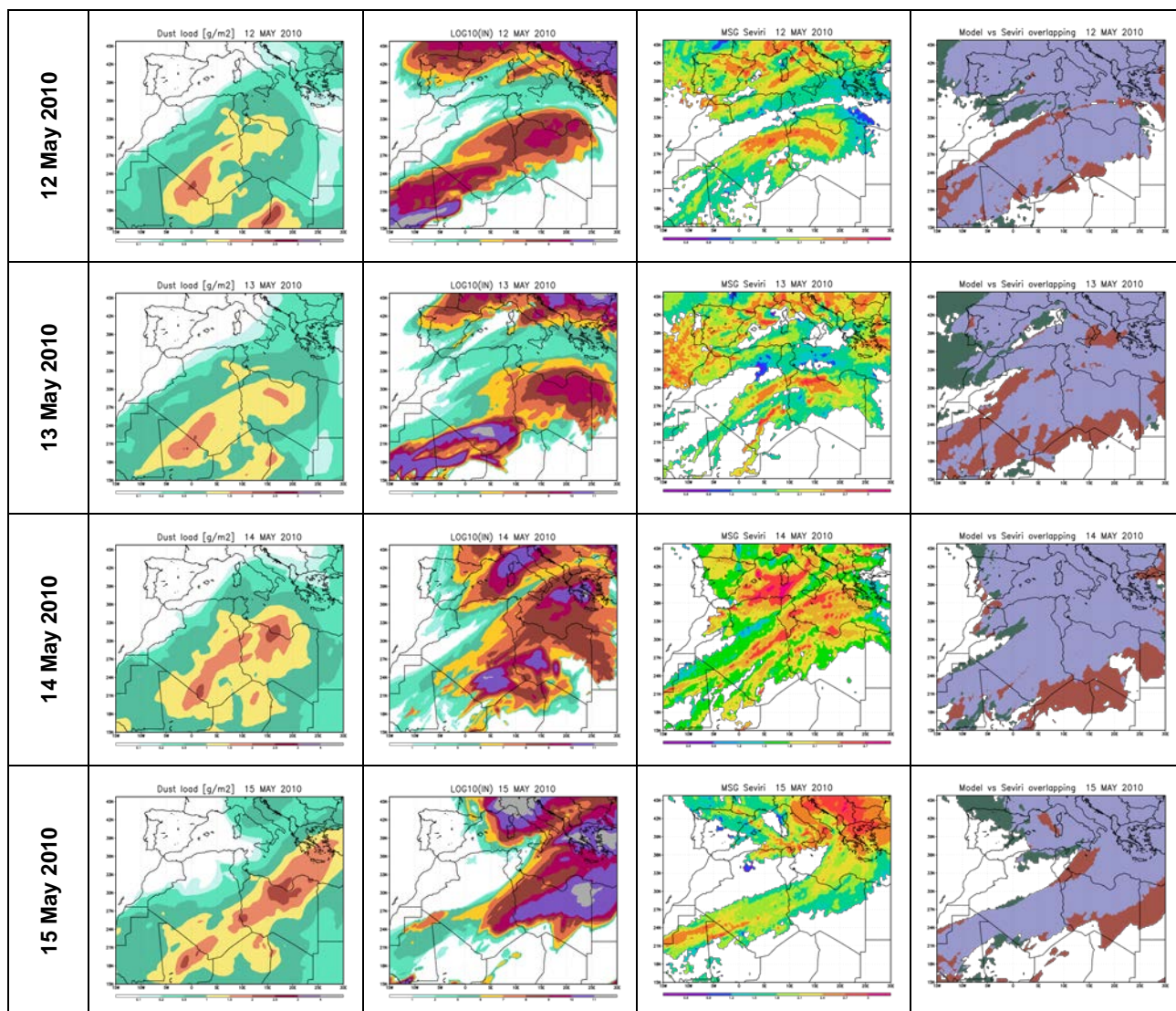


Figure 1: Daily-averages of (A) the model dust load (gm^{-2}); (B) the model $\text{NL} = \log_{10} \int n_{IN} dz$; (C) the MSG-SEVIRI $\text{IWPL} = \log_{10}(\text{IWP})$; (D) overlap of normalized NL and IWPL. The color selection: hits - blue; misses - green; false alarm – brown.

5

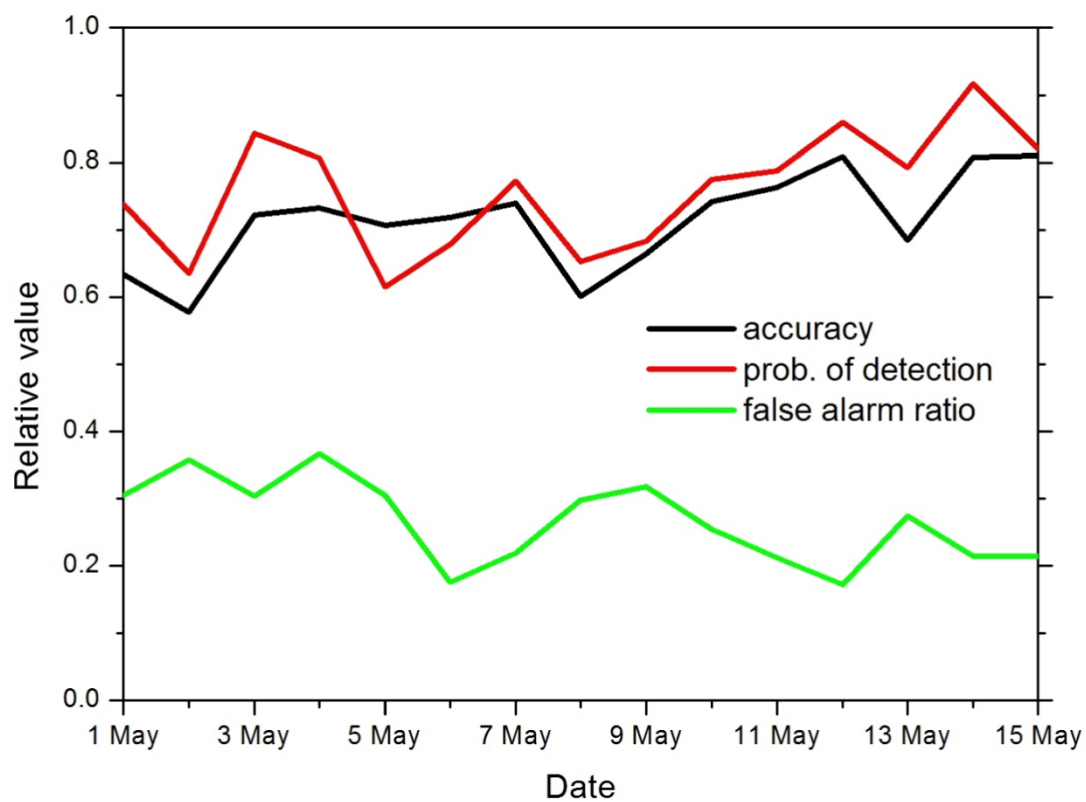


Figure 2: Time evolution of the forecast accuracy (black), the probability of detection (hit rate, red) and the false alarm ratio (green) for the period 1-15 May 2010.

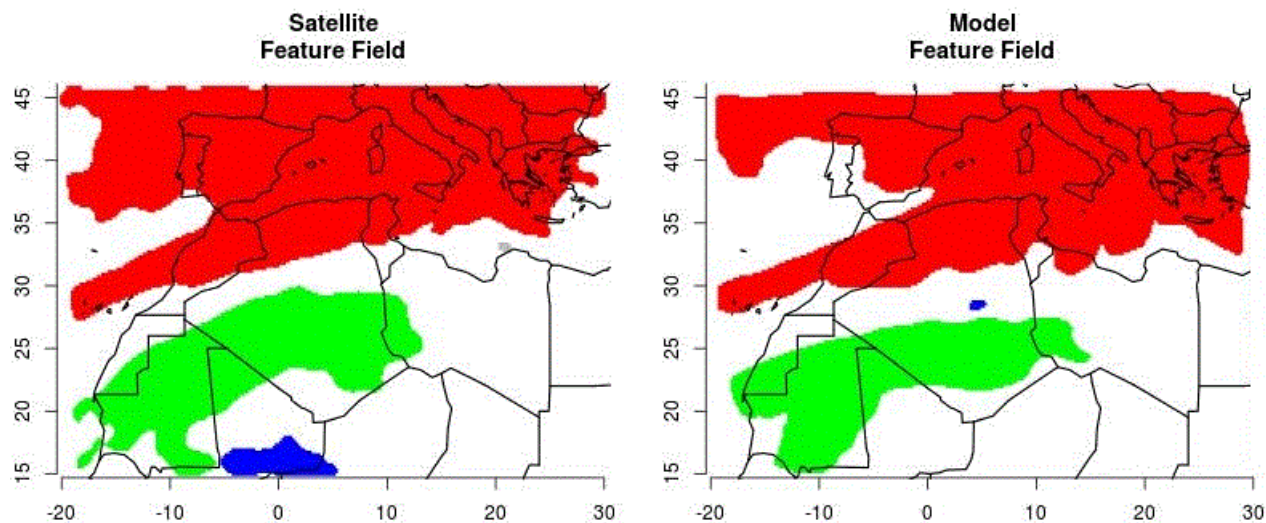


Figure 3: Best matching pairs of entities identified by the CRA feature matching technique when applied to normalized daily-averaged IWPL (left) and NL (right) fields valid for 11 May 2010.

5

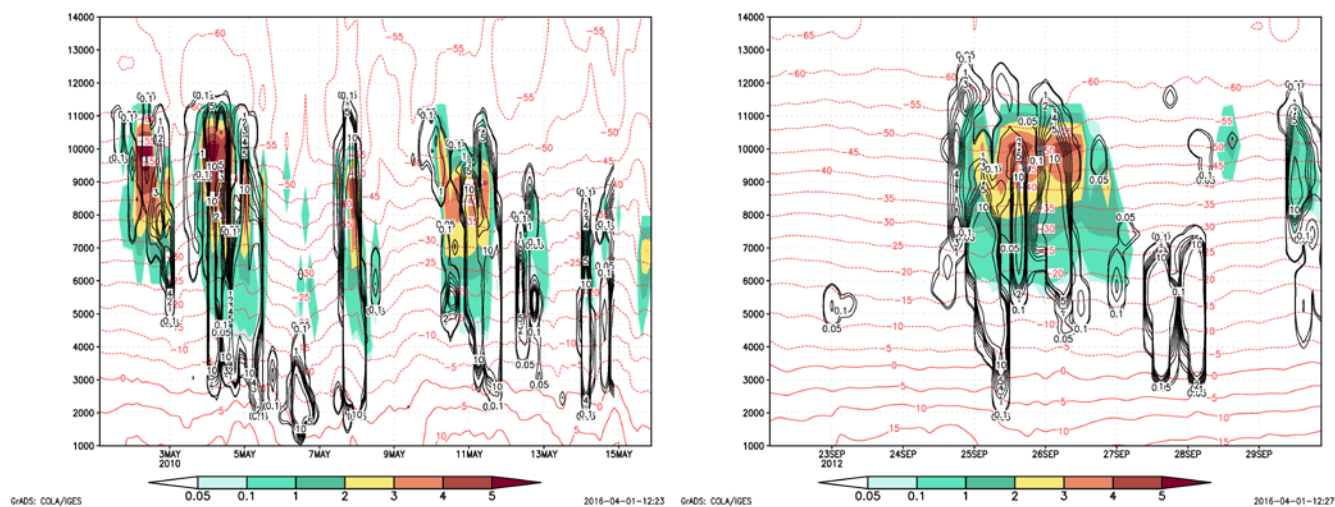


Figure 4: Comparison of $\log_{10}(\text{IWC} \times 10^{-6} \frac{\text{kg}}{\text{m}^3})$ obtained from Doppler radar reflectivity using Cloudnet algorithm (solid black line contour plot) versus DREAM $\log_{10}(n_{IN})$ (colored contour plot), in the period 1-15 May 2010 (A), and 22-30 September 2012 (B). Red contours show the temperature as provided by the NMME model.

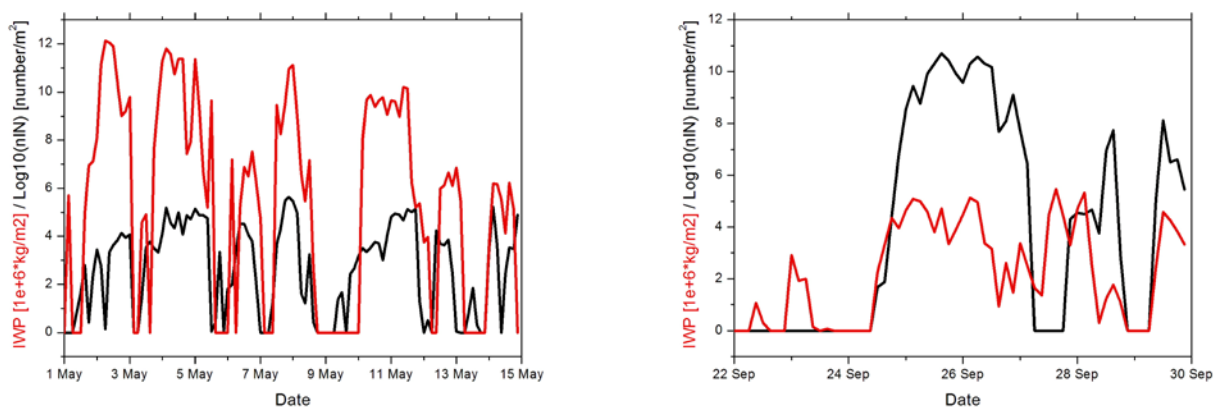
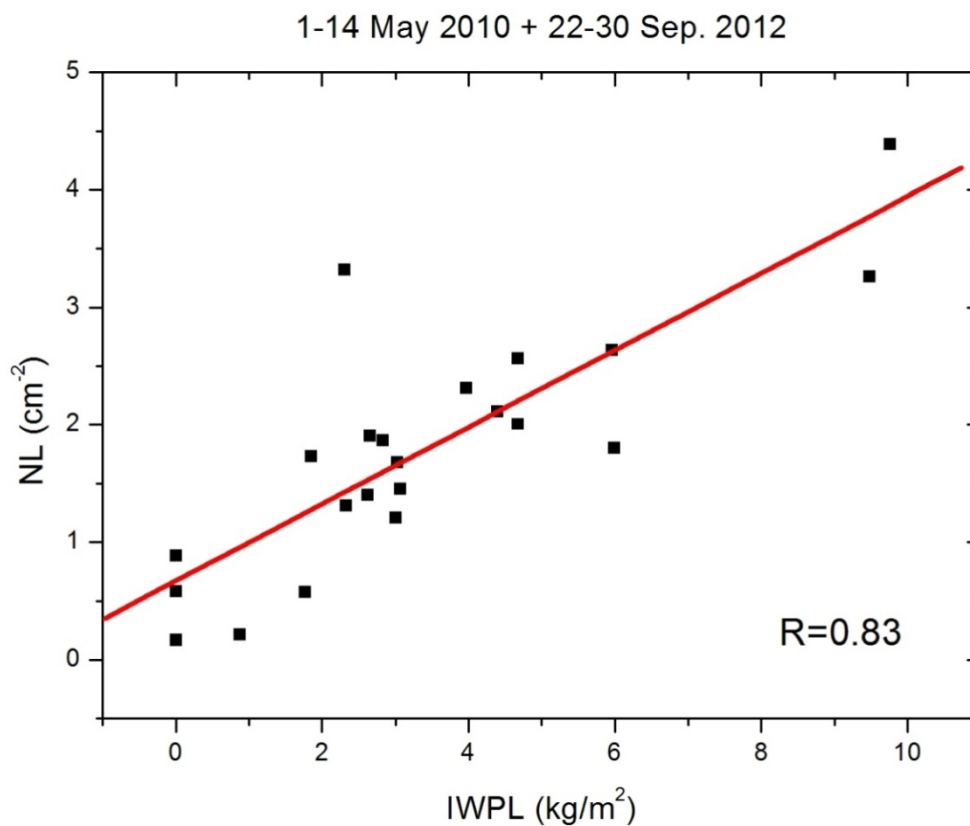


Figure 5: Time evolution of IWPL and NL over the period from 1-15 May 2010 (upper panel) and from 22-30 September 2012 (lower panel).



5 **Figure 6: Linear correlation between IWPL and NL retrieved using ground based measurements merging the datasets from both the selected cases studies of 1-15 May 2010 and 22-30 September 2012**